Original Article

ONO-1301, a Sustained-Release Prostacyclin Analog, Ameliorates the Renal Alterations in a Mouse Type 2 Diabetes Model Possibly Through Its Protective Effects on Mesangial Cells

Hiroyuki Watatani[a], Hiroko Yamasaki[a], Yohei Maeshima[a,b], Tatsuyo Nasu[a],
Norikazu Hinamoto[a], Haruyo Ujike[a], Hitoshi Sugiyama[a,c], Yoshiki Sakai[d],
Katsuyuki Tanabe[a]*, and Hirofumi Makino[a]

*Departments of [a]Medicine and Clinical Science, and [b]Chronic Kidney Disease and cardiovascular disease,
[c]Center for Chronic Kidney Disease and Peritoneal Dialysis, Okayama University Graduate School of Medicine,
Dentistry and Pharmaceutical Sciences, Okayama 700-8558, Japan, [d]ONO Pharmaceutical Co., Ltd., Osaka 541-8564, Japan*

Diabetic nephropathy is the most common pathological disorder predisposing patients to end-stage renal disease. Considering the increasing prevalence of type 2 diabetes mellitus worldwide, novel therapeutic approaches are urgently needed. ONO-1301 is a novel sustained-release prostacyclin analog that inhibits thromboxane A_2 synthase. Here we examined the therapeutic effects of the intermittent administration of slow-release ONO-1301 (SR-ONO) on diabetic nephropathy in obese type 2 diabetes mice, as well as its direct effects on mesangial cells. The subcutaneous injection of SR-ONO (3 mg/kg) every 3 wks did not affect the obesity or hyperglycemia in the *db/db* obese mice used as a model of type 2 diabetes, but it significantly ameliorated their albuminuria, glomerular hypertrophy, glomerular accumulation of type IV collagen, and monocyte/macrophage infiltration, and also the increase of TGF-β1, α-smooth muscle actin (α-SMA) and MCP-1 compared to vehicle treatment. In cultured mouse mesangial cells, ONO-1301 concentration-dependently suppressed the increases in TGF-β, type IV collagen, α-SMA, MCP-1 and fibronectin induced by high ambient glucose, at least partly through prostacyclin (PGI$_2$) receptor-mediated signaling. Taken together, these results suggest the potential therapeutic efficacy of the intermittent administration of SR-ONO against type 2 diabetic nephropathy, possibly through protective effects on mesangial cells.

Key words: prostacyclin, ONO-1301, diabetic nephropathy, TGF-β1, diabetes mellitus

Diabetic nephropathy is a major microvascular complication of type 1 and type 2 diabetes. Given the fact that diabetic nephropathy is the most common etiology predisposing subjects in developed countries to end-stage renal disease (ESRD), novel therapeutic approaches are urgently needed. Compared to type 1 nephropathy, type 2 diabetic nephropathy is more prevalent and has a more complex pathogenesis,

involving various comorbidities such as obesity, hypertension and dyslipidemia. Despite the differences in the underlying mechanisms of type 1 and type 2 diabetic nephropathy, the clinical and histological alterations are relatively similar, at least in the early stage. Glomerular hyperfiltration, glomerular hypertrophy and microalbuminuria are typically observed in the early stage of both types of diabetic nephropathy [1]. Subsequently, the expansion of the extracellular matrix (ECM) in mesangial areas and overt proteinuria are observed, eventually leading to glomerulosclerosis and ESRD [2].

The involvement of various factors and cytokines throughout the course of diabetic nephropathy, including the renin-angiotensin system, protein kinase C and advanced glycation end-products (AGEs) has been reported [3, 4]. Among them, the monocyte chemoattractant protein-1 (MCP-1) and fibrogenic transforming growth factor (TGF)-β1 produced by mesangial cells in the diabetic condition are particularly important factors in the progression of the nephropathy [3]. An increased expression of MCP-1 is associated with the infiltration of monocytes/macrophages into glomeruli, leading to inflammation and increased oxidative stress [5]. TGF-β1 expression causes mesangial ECM production, which possibly induces glomerulosclerosis [6].

Prostacyclin (PGI$_2$), a metabolite of arachidonic acid, possesses vasoprotective effects that includ antiplatelet aggregation, vasodilation and inhibition of smooth muscle cell proliferation [7, 8]. ONO-1301 is a synthetic nonprostanoid prostacyclin agonist that potently inhibits TXA$_2$ synthase [9]. ONO-1301 has been reported to have therapeutic effects in experimental models of pulmonary hypertension, pulmonary fibrosis and ischemic heart disease [9–11]. ONO-1301 polymerized with poly (D, L-lactic-co-glycolic acid) (PLGA) microspheres (ONO-1301MS) was developed as a sustained-release preparation to allow effective circulating levels to be maintained for 3 wks after a single subcutaneous injection [12].

The therapeutic effects of sustained-release ONO-1301MS (SR-ONO) have been demonstrated in experimental models of a variety of disorders, without causing hypotension, at doses up to 100 mg/kg [12–14]. The beneficial effect of ONO-1301 in treating cardiac ischemia was demonstrated to be partly mediated via the upregulation of hepatocyte growth factor

(HGF) and vascular endothelial growth factor (VEGF)-A, a potent pro-angiogenic factor, via a cAMP-dependent pathway [11, 15].

Hayashi *et al.* demonstrated that ONO-1301 (twice-daily administration) had antinephritic effects in a rat anti-GBM nephritis model by inhibiting intraglomerular leukocyte infiltration [16]. We also found that ONO-1301 had therapeutic effects in a rat type 1 diabetes model [17] and in a unilateral ureteral obstruction model [18]. However, the therapeutic effects of ONO-1301 on type 2 diabetic nephropathy, as well as the precise mechanism(s) involved in its renoprotective effects have been unclear. In the present study, we tested our hypothesis that SR-ONO may ameliorate the renal alterations in a representative type 2 diabetes model, the *db/db* mouse, by regulating the accumulation of the mesangial matrix, inflammation and oxidative stress through PGI$_2$ (IP) receptor-mediated signaling.

Materials and Methods

Mice.   We used adult male *db/db* mice (BKS. Cg-*db/db* Jcl; Clea Japan, Osaka, Japan) and their age-matched non-diabetic *db/*m littermates (BKS. Cg-*db/*+m Jcl; Clea Japan). The mice were given standard pellet laboratory chow and water *ad libitum*. The experimental protocol was approved by the Animal Care and Use Committee, Okayama University and complied with the "Guide for the Care and Use of Laboratory Mice" (NIH publication No. 86–23, revised 1985).

Preparation of slow-release ONO-1301 (SR-ONO).   ONO-1301 was synthesized by ONO Pharmaceutical Co. Ltd. (Osaka, Japan) as described [10, 19]. The sustained-release form of ONO-1301 (SR-ONO) was generated by polymerizing ONO-1301 with poly-lactic and glycolic acid (PLGA) as described [12, 13]. The mean particle dia of SR-ONO was 4.5 $\pm 0.3 \mu$m as determined by a laser diffraction particle size analyzer (model SALD-2100; Shimadzu, Kyoto, Japan). The release time was adjusted to 25 days, as determined by measuring the residual ONO-1301 in the pellets by high-performance liquid chromatography (HPLC) [12].

Protocol for animal experiments.   We used 8-wk-old *db/db* mice, because they develop hyperglycemia at 7–8 weeks of age. The blood glucose level of

the 8-wk-old *db/db* mice was in the range of 19.4–26.2 mmol/l. The mice were divided into 3 subgroups (n = 6 for each subgroup): (1) non-diabetic control *db/m* mice, *db/db* mice treated with either (2) vehicle (PLGA polymer containing no active substance), or (3) SR-ONO at a dose of 3 mg/kg body weight. The vehicle or SR-ONO was subcutaneously injected on the mouse's back every 3 wks. At 8 wks after the initial injection of SR-ONO (when the mice were 16 wks old), the mice were anesthetized via an intraperitoneal injection of 50 mg/kg body weight of pentobarbital sodium (Sigma, St. Louis, MO, USA), they were sacrificed and their kidneys were removed. No mice died before the sacrifice, and no signs of any apparent exhaustion were observed during the experimental period.

Blood and urine examination. The blood glucose level was measured in tail-vein blood using a conventional glucometer, and individual 24-h urine sample collections were performed using metabolic cages at 8-wks after the initial administration of SR-ONO. Non-fasting blood samples were drawn from the retro-orbital venous plexus using heparinized capillary tubes under anesthesia at the time of sacrifice. The serum and urinary creatinine levels and concentrations of urinary albumin were measured by Okayama Medical Laboratories (OML; Kurashiki, Japan) using HPLC, an enzymatic colorimetric assay and an enzyme-linked immunosorbent assay (ELISA), respectively. The urinary albumin concentrations were normalized to the urinary creatinine levels, and they are expressed as the urinary albumin/creatinine ratio (UACR). The creatinine clearance (Ccr) was calculated and is expressed as ml/min. The plasma levels of total cholesterol and urea nitrogen at 8 wks after the initial administration of SR-ONO were also measured by OML. The serum levels of ONO-1301 at 2 wks after the final injection of vehicle or SR-ONO were measured by liquid chromatography tandem mass spectrometry assay as described [12].

Histological analysis. At 8 wks after the start of the treatment, the kidneys were removed from the mice, fixed in 10% buffered formalin and embedded in paraffin. Sections (3-μm) were stained with periodic acid-Schiff (PAS) for light microscopic observation [20]. The mean glomerular tuft volume (G_V) was determined from the mean glomerular cross-sectional tuft area (G_A) as described previously [21, 17]. We observed 20 glomeruli from each cortical area, and images were taken and analyzed using the Lumina Vision software program (Mitani, Fukui, Japan) to determine the mean G_A. The G_V was calculated as $G_V = \beta/k \times (G_A)^{3/2}$, with $\beta = 1.38$, the shape coefficient for spheres, and k = 1.1, a size distribution coefficient [21]. G_V is expressed relative to the value of the non-diabetic control group.

We defined the mesangial matrix index as the proportion of G_V occupied by the mesangial matrix, excluding nuclei. The mesangial matrix areas of 20 glomeruli in each kidney were analyzed and averaged as described [22]. The mesangial areas were selected using the Photoshop software program (Adobe Systems, San Jose, CA, USA), followed by analysis using the Lumina Vision software program.

Immunohistochemistry. The immunohistochemical studies were performed using paraffin-embedded sections as described previously [23–25]. After deparaffinization and rehydration, the sections were incubated with 3% H_2O_2 in methanol to inactivate endogenous peroxidase. The sections were boiled in citrate buffer (10 mM citric acid and 0.05% Tween 20 [pH 6.0]) for antigen retrieval. The sections were then blocked with phosphate-buffered saline (PBS) containing 3% bovine serum albumin (BSA) and an avidin/biotin Blocking Kit (Vector Laboratories, Burlingame, CA, USA), followed by incubation with rat polyclonal anti-F4/80 (1 : 200 dilution, Serotec, Oxford, UK) or mouse monoclonal anti-malon dialdehyde (MDA; 1 : 100, NOF Corp., Tokyo, Japan) antibodies. The sections were then incubated with biotinylated secondary antibodies (Nichirei, Tokyo, Japan), and immunoperoxidase staining was conducted utilizing a Vectastain ABC Elite Reagent kit (Vector Laboratories). Biotinylated goat anti-rat IgG for F4/80 (1 : 100 dilution) was used as secondary antibody. A M.O.M.™ kit (Vector Laboratories) was used for the staining with the mouse monoclonal anti-MDA antibody. Diaminobenzidine (DAB) was used as a chromogen. All slides were counterstained with hematoxylin. Normal mouse or rabbit IgG was used as a negative control.

The number of glomerular F4/80$^+$ monocytes/macrophages in each glomerulus was determined. To evaluate the MDA-positive area, we obtained color images as TIFF files and analyzed then using the Lumina Vision software program. Image files (TIFF)

were opened in the gray-scale mode. The MDA-positive area was calculated using the following formula: $[\text{X (density)} \times \text{positive area } (\mu m^2)]/\text{glomer-ular total area } (\mu m^2)$, where the staining density is indicated by a number from 0 to 256 in the gray scale [17]. We examined 40 glomerular cross-sections in each kidney. Histological evaluations were performed in a blinded fashion by 2 investigators, and the results were averaged.

Immunofluorescence. Immunofluorescent staining was performed as described [23, 26]. Briefly, frozen sections were fixed in cold ($-20\,°C$) acetone for 10 min and then air-dried. The sections were blocked with 1% BSA and then incubated with poly-clonal rabbit anti-type IV collagen (1:100 dilution, Chemicon, Billerica, MA, USA) for 1 h. Subsequently, the sections were washed three times in PBS and incubated with Alexa Fluor 488-labeled goat anti-rabbit IgG (Invitrogen, Carlsbad, CA, USA) for 1 h. After three washes with PBS, Vectashield anti-fade mounting medium (Vector Laboratories) was applied and the sections were observed by fluorescence microscopy (BZ-Analyzer; Keyence, Osaka, Japan) and images were obtained. Normal rabbit IgG was used as a negative control. To assess the positive area, we analyzed the image files ($1,392 \times 1,040$ pix-els) at $\times 400$ magnification using the Lumina Vision software program.

Immunoblotting. Immunoblotting was per-formed as described [23, 27, 28]. Briefly, tissues were homogenized in radioimmunoprecipitation assay buffer at $4\,°C$. After centrifugation at 14,000 rpm for 30 min at $4\,°C$, the supernatant was collected and stored at $-80\,°C$ until use. The total protein concen-tration was determined by the DC-protein determina-tion system (Biorad, Hercules, CA, USA) using BSA as a standard. The samples were processed for sodium dodecyl sulfate-polyacrylamide gel electropho-resis (SDS-PAGE), and the proteins were electro-transferred onto nitrocellulose membranes (Invitrogen).

The membranes were blocked with 5% non-fat dry milk in 1X Tris-buffered saline containing 0.1% Tween-20 for 1 h, incubated over night with polyclonal rabbit anti-type IV collagen (1:20 dilution, Southern Biotech, Birmingham, AL, USA), anti-TGF-β (1:20 dilution), alpha-smooth muscle actin (α-SMA; 1:50 dilution, Chemicon), and Armenian hamster anti-mouse MCP-1 (1:250 dilution; BioLegend, San Diego, CA, USA) antibodies at $4\,°C$. After incubation with horse-radish peroxidase-labeled anti-rabbit IgG antibodies for TGF-$\beta 1$ or anti-hamster IgG antibodies for MCP-1 for 1 h, we detected the signals using an enhanced chemiluminescence system (Amersham, Arlington Heights, IL, USA). The membranes were re-probed with rabbit anti-actin antibodies (Chemicon) to serve as loading controls. The density of each band was determined using the NIH Image J software pro-gram, and the density is expressed as a value relative to the density of the corresponding band obtained from the actin immunoblot.

Real-time PCR. RNA extraction, reverse transcription-polymerase chain reaction (RT-PCR) and quantitative real-time PCR were performed as described [23, 29]. Tissues or cells were homoge-nized, and the total RNA was extracted using an RNeasy Midi Kit (Qiagen, Chatsworth, CA, USA) for *in vivo* assays or an RNeasy Mini Kit (Qiagen) for *in vitro* assays, and the samples were stored at $-80\,°C$ until use. The total RNA was subjected to RT with poly-d (T) primers and reverse transcriptase (RTG T-Primed First-Strand kit; Amersham Pharmacia Biotech, Piscataway, NJ, USA). Quantitative real-time PCR was used to quantify the amounts of TNF-α, TGF-$\beta 1$, MCP-1 and fibronectin mRNA. cDNA was diluted 1:5 with autoclaved deionized water, and $5\,\mu l$ of the diluted cDNA was added to Lightcycler Mastermix, $0.5\,\mu mol/l$ of specific primers, $3\,mmol/l$ $MgCl_2$ and $2\,\mu l$ of Master SYBR Green (Roche Diagnostics, Mannheim, Germany). This reac-tion mixture was filled up to a final volume of $15\,\mu l$ with water. PCR was carried out in a real-time PCR cycler (Lightcycler; Roche Diagnostics).

The program was optimized and finally performed as: denaturation at $95\,°C$ for 10 min, followed by 60 cycles of amplification for MCP-1 ($95\,°C$ for 10 sec, $68\,°C$ for 10 sec and $72\,°C$ for 16 sec), 50 cycles of amplification for TNF-α and fibronectin (TNF-α: $95\,°C$ for 10 sec, $60\,°C$ for 10 sec and $72\,°C$ for 10 sec, fibronectin: $95\,°C$ for 10 sec, $62\,°C$ for 10 sec and $72\,°C$ for 8 sec), 45 cycles of amplification for TGF-β ($95\,°C$ for 10 sec, $60\,°C$ for 10 sec and $72\,°C$ for 8 sec) and 40 cycles of amplification for 18S rRNA ($95\,°C$ for 10 sec, $68\,°C$ for 10 sec and $72\,°C$ for 16 sec). The temperature ramp rate was $20\,°C$ per sec. At the end of each extension step, the fluorescence was measured to quantify the PCR products.

After completion of the PCR, we measured the melting curve of the product by using the temperature gradient from 65℃ to 95℃ at 0.2℃ per sec, with continuous fluorescence monitoring to produce a melting profile of the primers. The amount of PCR products was normalized to that of 18S rRNA to determine the relative expression ratio for the mRNA. The following oligonucleotide primers specific for mouse TNF-α, TGF-β1, MCP-1, fibronectin and 18S rRNA were used:

TNF-α: 5'-GTTCTATGGCCCAGACCCTCAC-3' (forward)
and 5'-GGCACCACTAGTTGGTTGTCTTTG-3' (reverse);
TGF-β1: 5'-GTGTGGAGCAACATGTGGAACT CTA-3' (forward)
and 5'-TTGGTTCAGCCACTGCCGTA-3' (reverse);
MCP-1: 5'-AGGTCCCTGTCATGCTTCT-3' (forward)
and 5'-CTGCTGGTGATCCTCTTGT-3' (reverse);
fibronectin; 5'-GCTTTGGCAGTGGTCATTTCAG -3' (forward)
and 5'-ATTCCCGAGGCATGTGCAG-3' (reverse);
18S rRNA: 5'-TTCTGGCCAACGGTCTAGACAA C-3' (forward)
and 5'-CCAGTGGTCTTGGTGTGCTGA-3' (reverse).

In vitro experiments.   Primary murine mesangial cells (Mes13) were purchased from the ATCC (Rockville, MD, USA). Mesangial cells were used between the 10th and 20th passage. The characteristics of mesangial cells were confirmed by immunoreactivity for actin and desmin and a lack of staining for factor VIII, as described previously [30]. The cells were cultured in Dulbecco's modified Eagle's medium (DMEM; Sigma, St. Louis, MO, USA) containing 10% fetal calf serum (FCS; Cansera International, Etobicoke, Ontario, Canada), 100 U/mL penicillin and 100 μg/mL streptomycin at 37℃. After they become subconfluent, we starved the cells for 24h by incubating them in DMEM containing 0.2% FCS.

The resulting quiescent cells were incubated with 5.5 mM normal glucose (NG), NG with 19.5 mM mannitol (NG/Manni), 25 mM high glucose (HG) with PBS-DTT buffer (HG/N0), HG with ONO-1301 at 1 nM (HG/O1), 10 nM (HG/O10) or 100 nM (HG/ O100) for 6h (for real-time PCR) or 12h (for immunoblotting). We determined the concentration of mannitol (19.5 mM) in order to set the osmotic pressure of the NG group (5.5 mM) equivalent to that of the HG group (25 mM). In another set of experiments performed to assess the involvement of the PGI$_2$ (IP) receptor, we incubated the quiescent Mes13 cells with HG with 100 nM ONO-1301 in the presence of a selective PGI$_2$ (IP) receptor antagonist CAY10449 (Cayman Cehemical, Ann Arbor, MI, USA) at a concentration of 0, 10 or 100 nM. The cells were then harvested and subjected to immunoblotting or real-time PCR analyses.

Statistical analysis.   All values are expressed as the means $\pm$ SEM. The results were analyzed using a one-way analysis of variance (ANOVA), followed by Tukey's post-hoc test, when the data were parametric. If necessary, the data were analyzed with a nonparametric Kruskal-Wallis test, followed by a Steel-Dwass multiple comparisons test. A value of $p < 0.05$ was considered significant. All statistical tests were performed using the JMP version 9 software package (SAS Institute, Cary, NC, USA).

Results

Changes in blood glucose, lipids and renal function.   The diabetic db/db mice treated with vehicle exhibited hyperglycemia throughout the experimental period. Treatment with SR-ONO did not affect the hyperglycemia in the diabetic mice (Table 1). Similarly, SR-ONO treatment did not significantly affect the plasma levels of total cholesterol, BUN or creatinine in the diabetic mice (Table 1). The diabetic db/db mice treated with the vehicle exhibited higher body weights and visceral fat weights (peritesticular fat weight adjusted by body weight) at 8 wks compared to the non-diabetic mice, and treatment with SR-ONO did not significantly influence these parameters in the diabetic mice (Table 1).

Serum levels of ONO-1301.   Previous studies demonstrated that the subcutaneous injection of SR-ONO resulted in stable circulating levels of ONO-1301 for 3 wks [12, 17, 18]. In the present study, the serum levels of ONO-1301 were significantly elevated in the SR-ONO-treated mice, whereas the concentration of ONO-1301 was below the limit of detection in the non-diabetic mice and in the vehicle-treated diabetic mice (Fig. 1A).

Changes in creatinine clearance and urinary

albumin excretion.   The diabetic mice treated with the vehicle showed a marked elevation of Ccr and UACR compared to the non-diabetic control mice. Treatment with SR-ONO did not significantly affect the elevation of Ccr (Fig. 1B), but significantly suppressed the increase in the UACR compared to the vehicle treatment in diabetic mice (Fig. 1C).

Histology and morphometric analysis.   The glomerular hypertrophy observed in the vehicle-treated *db/db* mice was mildly suppressed by SR-ONO treatment, and the mesangial matrix expansion observed in the vehicle-treated diabetic mice was also reduced by SR-ONO treatment (Fig. 2A–C). A morphometric analysis (Fig. 2D, E) further confirmed the

presence of significant inhibitory effects of SR-ONO on these parameters. In the diabetic mice, tubulointerstitial injuries were not evident on PAS-stained sections.

Immunohistochemical analysis of glomerular type IV collagen.   We next examined the accumulation of glomerular type IV collagen by immunofluorescence (Fig. 3). The amount of type IV collagen in the glomeruli was increased in the vehicle-treated diabetic mice (Fig. 3B) compared to the non-diabetic mice (Fig. 3A). Enhanced immunoreactivity in the diabetic mice was observed mainly in the glomerular and tubular basement membrane, Bowman's capsule and in the mesangial area. Treatment with SR-ONO

Table 1   Clinical parameters of the three treatment groups

	db/m	*db/db* (vehicle)	*db/db* (SR-ONO)
Body weight (g)	28.4 ± 0.4	$46.1 \pm 0.8^*$	$49.0 \pm 3.3^*$
Peritesticular fat weight (mg/g body weight)	15.9 ± 2.6	$56.2 \pm 5.2^*$	$60.5 \pm 2.2^*$
Blood pressure SBP/DBP (mmHg)	$122 \pm 3/76 \pm 4$	$121 \pm 2/74 \pm 4$	$117 \pm 3/72 \pm 3$
Blood glucose (mg/dL)	119 ± 2	$590 \pm 5^*$	$579 \pm 9^*$
BUN (mg/dL)	18.0 ± 1.4	23.0 ± 4.0	18.1 ± 1.8
Serum creatinine (mg/dL)	0.117 ± 0.015	$0.063 \pm 0.006^*$	$0.047 \pm 0.009^*$
Total cholesterol (mg/dL)	78.0 ± 1.5	$119.8 \pm 5.8^*$	$122.2 \pm 3.4^*$

$^*p < 0.01$ vs. *db*/m. The values are shown as the means $\pm$ SEM. N = 6 in each group. BUN, blood urea nitrogen; SR-ONO, slow-release form of ONO-1301; SBP/DBP, systolic BP/diastolic BP.

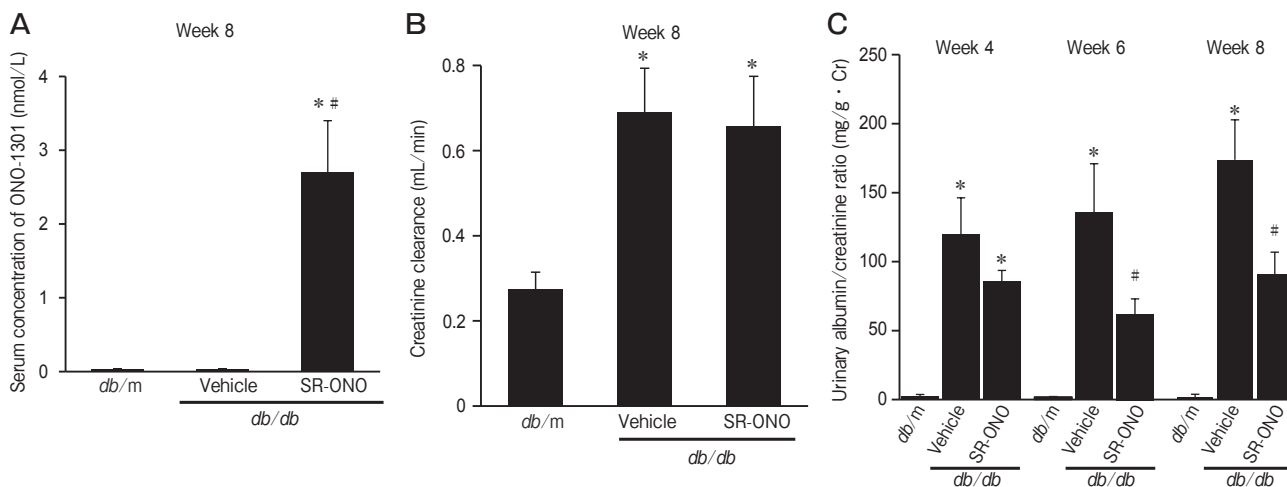**Fig. 1**   (**A**) The serum levels of ONO-1301 were undetectable in the non-diabetic mice and the vehicle-treated *db/db* mice. In the *db/db* mice treated with SR-ONO, a significant elevation of the serum levels of ONO-1301 was observed. (**B**) The increase in the Ccr in the *db/db* mice was not affected by treatment with SR-ONO. (**C**) The urinary albumin/creatinine ratio (UACR). The increase in the UACR was significantly suppressed by treatment with SR-ONO (10 mg/kg, every 3 wks) compared to the vehicle treatment. The data obtained at the end of the experimental period are shown. $^*p < 0.01$ vs. non-diabetic mice. $^\#p < 0.01$ vs. diabetic mice. n = 6 in each group. Each column shows the means $\pm$ SE. SR-ONO, slow-release form of ONO-1301.
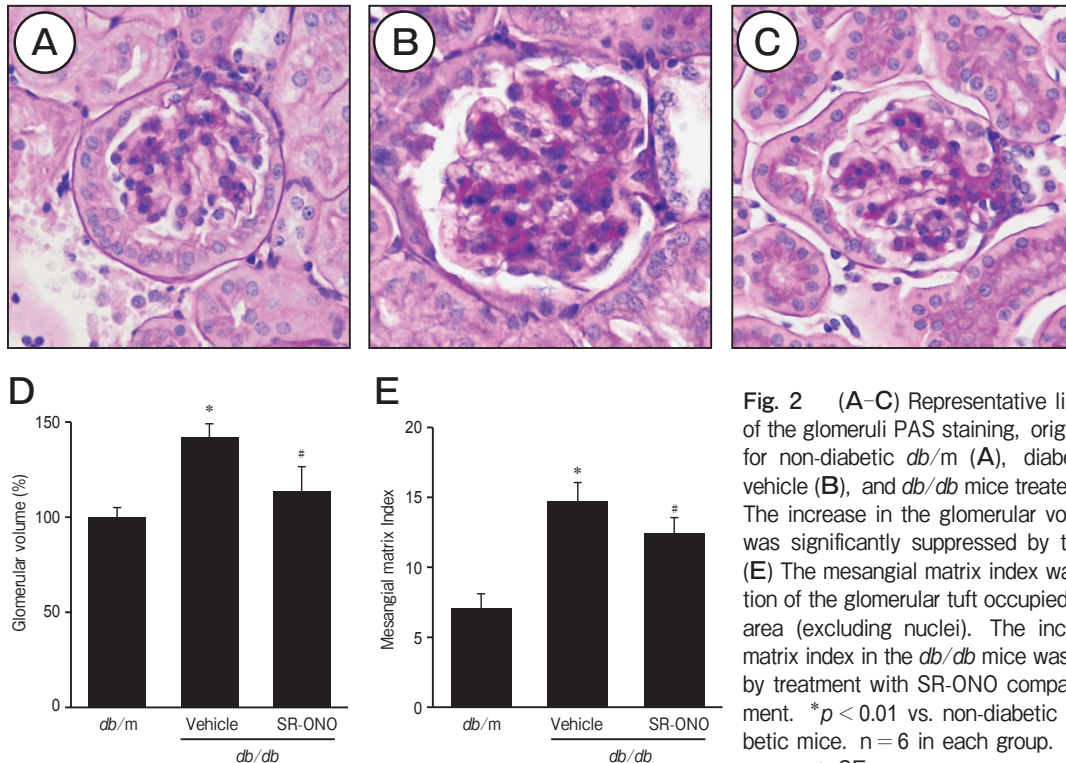
Fig. 2   (A–C) Representative light microscopic findings of the glomeruli PAS staining, original magnification ×400) for non-diabetic db/m (A), diabetic db/db treated with vehicle (B), and db/db mice treated with SR-ONO (C). (D) The increase in the glomerular volume in the db/db mice was significantly suppressed by treatment with SR-ONO. (E) The mesangial matrix index was defined as the proportion of the glomerular tuft occupied by the mesangial matrix area (excluding nuclei). The increase in the mesangial matrix index in the db/db mice was significantly suppressed by treatment with SR-ONO compared to the vehicle treatment. $^*p < 0.01$ vs. non-diabetic mice. $^{\#}p < 0.01$ vs. diabetic mice. n = 6 in each group. Each column shows the means ± SE.

(Fig. 3C) decreased the accumulation of type IV collagen in the db/db mice compared to the vehicle treatment, and these results were confirmed by a quantitative morphometric analysis (Fig. 3D). We further evaluated the expression of type IV collagen in the renal cortex by performing an immunoblot analysis. Again, the increases in the protein levels of type IV collagen in the db/db mice were significantly prevented by the treatment with SR-ONO (Fig. 3E).

Renal levels of TGF-β and α-SMA.   TGF-$β$1 is a pro-fibrotic factor involved in the mesangial matrix expansion and renal hypertrophy in diabetic nephropathy [31]. The present immunoblot analysis for TGF-$β$1 revealed that the levels of TGF-$β$1 were increased in the vehicle-treated diabetic mice compared to the non-diabetic mice (Fig. 4A, B). Treatment with SR-ONO significantly prevented this increase in the levels of TGF-$β$ in the db/db mice compared to the vehicle treatment (Fig. 4A, B).

In diabetic glomeruli, the mesangial cells express $α$-SMA in association with the phenotypic alteration of these cells, leading to the excessive accumulation of mesangial matrix. We therefore examined the protein levels of $α$-SMA by an immunoblot analysis. The lev-

els of $α$-SMA were increased in the vehicle-treated diabetic mice compared to the non-diabetic mice (Fig. 4A, C). Treatment with SR-ONO significantly suppressed the elevation of $α$-SMA compared to the vehicle treatment (Fig. 4A, C).

Monocyte/macrophage infiltration and the expression of MCP-1/TNF-α.   We next examined the glomerular infiltration of monocytes/macrophages by performing an immunohistochemical study of F4/80. In the vehicle-treated diabetic mice (Fig. 5B), the number of glomerular F4/80$^+$ cells was significantly increased compared to that in the non-diabetic mice (Fig. 5A). Treatment with SR-ONO (Fig. 5C) markedly suppressed the accumulation of monocytes/macrophages in the glomeruli compared to the vehicle treatment (Fig. 5D).

Monocytes/macrophages are recruited by the local expression of MCP-1. TNF-$α$, a well-known proinflammatory cytokine, is also involved in microinflammation and in the pathogenesis of diabetic nephropathy. The increases in the levels of MCP-1 in the diabetic kidneys were significantly suppressed by the treatment with SR-ONO, as shown by the results of the immunoblot and real-time PCR analyses (Figs.
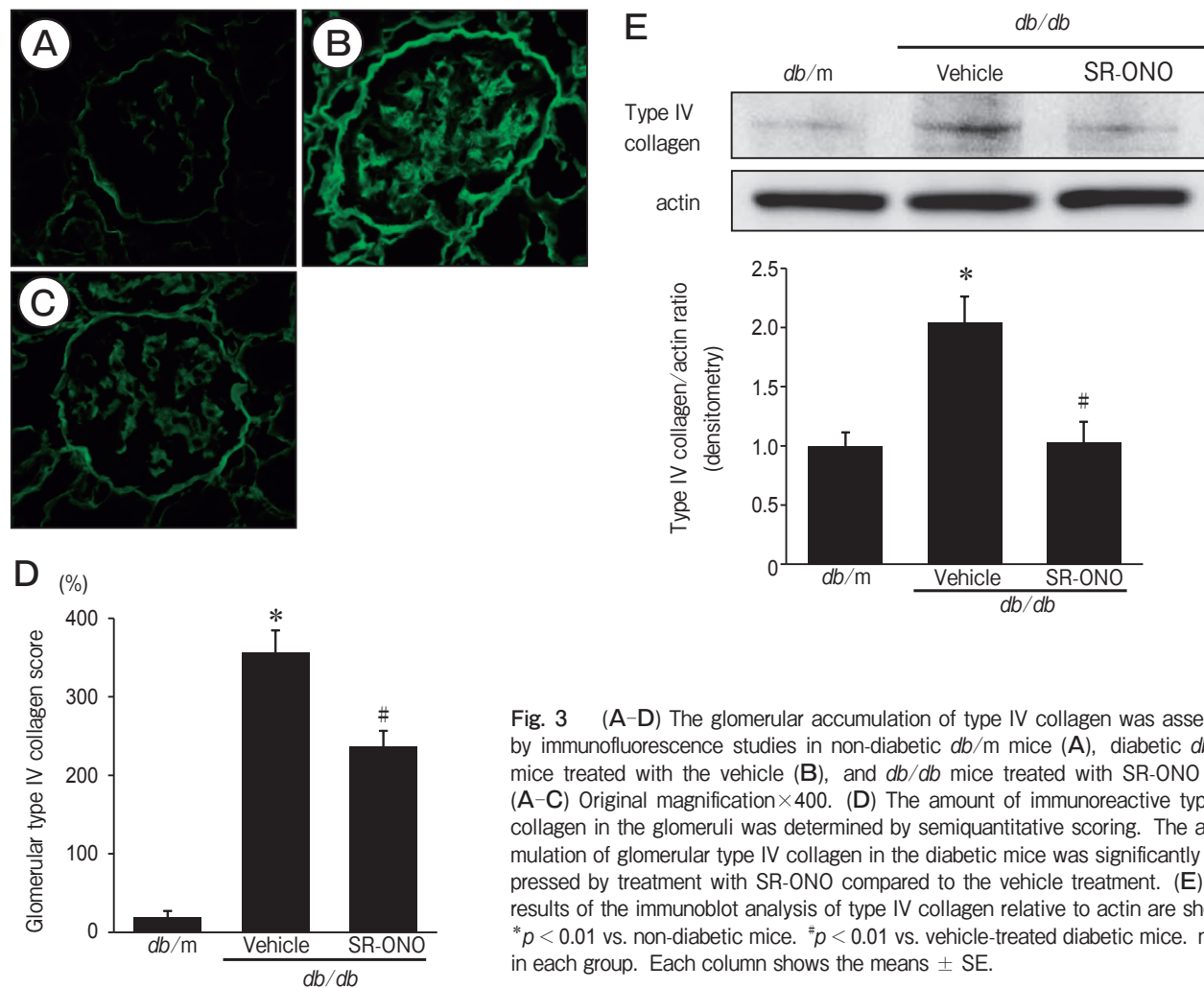
Fig. 3   (**A–D**) The glomerular accumulation of type IV collagen was assessed by immunofluorescence studies in non-diabetic *db*/m mice (**A**), diabetic *db*/*db* mice treated with the vehicle (**B**), and *db*/*db* mice treated with SR-ONO (**C**). (**A–C**) Original magnification×400. (**D**) The amount of immunoreactive type IV collagen in the glomeruli was determined by semiquantitative scoring. The accumulation of glomerular type IV collagen in the diabetic mice was significantly suppressed by treatment with SR-ONO compared to the vehicle treatment. (**E**) The results of the immunoblot analysis of type IV collagen relative to actin are shown. *$p < 0.01$ vs. non-diabetic mice. #$p < 0.01$ vs. vehicle-treated diabetic mice. n = 6 in each group. Each column shows the means ± SE.

5E, F). Similarly, the increase in the level of TNF-α mRNA in the renal cortex of the *db*/*db* mice was significantly inhibited by the treatment with SR-ONO compared to the vehicle treatment (Fig. 5G).

Immunohistochemical analysis of glomerular oxidative stress.   We next analyzed the glomerular accumulation of oxidative stress-related substances. The localization of MDA-positive areas was mainly in podocytes. The glomerular accumulation of MDA was markedly increased in the *db*/*db* mice (Fig. 6B) compared to the *db*/m mice (Fig. 6A). SR-ONO treatment significantly suppressed the glomerular accumulation of these substances (Fig. 6C), as confirmed by a quantitative morphometric analysis (Fig. 6D). These results suggest that macrophage infiltration might cause an increased in the glomerular oxidative stress,

leading to podocyte damage and subsequent albuminuria, and that treatment with SR-ONO effectively suppressed this cascade.

Fibrotic and inflammatory protein expression in cultured mesangial cells.   We performed *in vitro* experiments using mouse mesangial cells (Mes13) to examine the direct effects of SR-ONO on the expression of fibrotic and inflammatory proteins under the high-glucose (HG) condition. The immunoblotting and real-time PCR analyses demonstrated that the profibrotic TGF-β1 expression was markedly increased under the HG condition compared to the normal glucose condition, and SR-ONO significantly suppressed its expression in a concentration-dependent manner (Fig. 7A, B). The HG-induced α-SMA expression in mesangial cells, suggesting the altera-
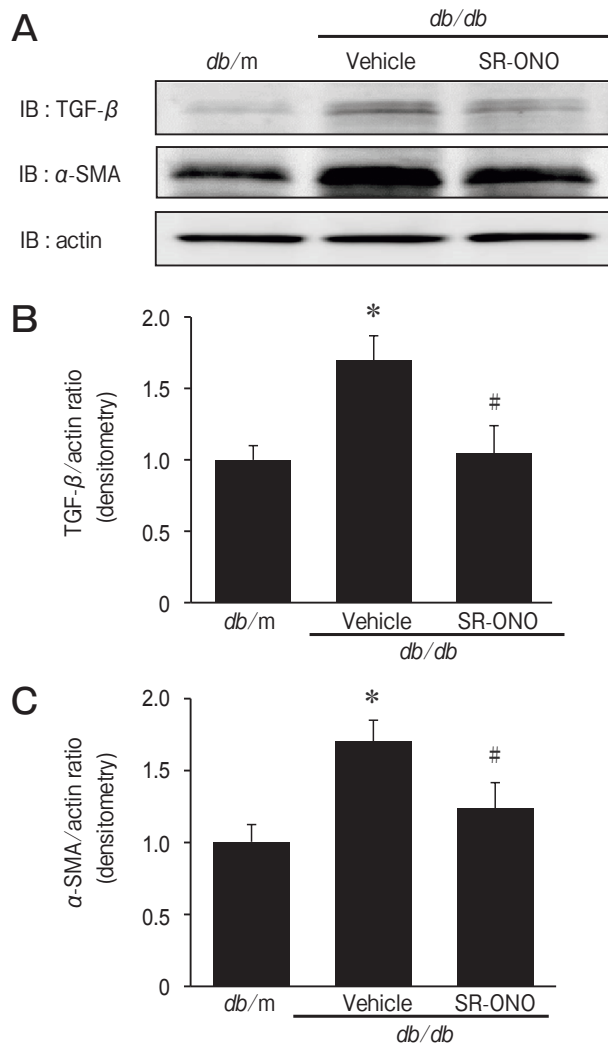
Fig. 4 The results of the immunoblot analyses of TGF-β1 and α-SMA. (**A**) The expression levels of TGF-β1 (**B**) and α-SMA (**C**) were determined by immunoblotting for non-diabetic controls, diabetic mice treated with vehicle and diabetic mice treated with SR-ONO. The intensities relative to actin based on the densitometry data are shown. The expression levels of both molecules were markedly increased in the vehicle-treated db/db mice compared to the db/m mice, and were significantly suppressed by SR-ONO. $^*p$ < 0.01 vs. non-diabetic animals. $^\#p$ < 0.01 vs. vehicle-treated diabetic animals. n = 6 in each group. Each column shows the means ± SE.

tion of the cell's phenotype into activated mesangial cells [32], was significantly suppressed by treatment with SR-ONO (Fig. 7C). The increased production of type IV collagen and fibronectin in the mesangial cells cultured in the HG condition was also inhibited by SR-ONO (Figs. 7C–F). The increase in the MCP-1

expression under the HG condition was also significantly prevented by SR-ONO treatment, in a concentration-dependent manner (Fig. 7G. These findings suggest that SR-ONO may directly act on mesangial cells to inhibit the accumulation of ECM and the infiltration of macrophages.

Lastly, we examined whether these therapeutic effects of SR-ONO were mediated by the PGI$_2$ (IP) receptor expressed on mesangial cells, by using a selective IP receptor antagonist, CAY10449. The inhibitory effects of SR-ONO on the expression of TGF-β1 and MCP-1 were significantly reversed by treatment with CAY10449 (Fig. 8A, B), suggesting that IP receptor signaling has a crucial role in mediating the therapeutic effects of SR-ONO.

Discussion

We demonstrated herein that the administration of slow-release ONO-1301MS ameliorated the glomerular injury and albuminuria in a mouse model of type 2 diabetic nephropathy. ONO-1301 is a synthetic prostacyclin agonist possessing potent inhibitory activity against TXA$_2$ synthase [9]. The therapeutic effects of prostacyclin and its analogues have been demonstrated for several disease conditions, including myocardial ischemia [33] and pulmonary arterial hypertension [34]. In addition, beraprost sodium, a prostacyclin analogue, has been shown to have therapeutic effects against proteinuria and glomerular injuries in both the streptozotocin (STZ)-induced type 1 diabetic and obese OLETF type 2 diabetic rat models [35, 36]. TXA$_2$ has been considered to be a critical mediator of the diabetic endothelial dysfunction, as well as renal injury, probably via its regulation of renal oxidative stress. The therapeutic effects of a thromboxane receptor antagonist, S18886, were reported in STZ-induced diabetic apolipoprotein E-deficient mice [37] and in obese Zucker type 2 diabetic rats [38]. These findings suggest that ONO-1301 may be a promising therapeutic agent for diabetic nephropathy.

The pathogenesis of type 2 diabetic nephropathy has been found to be extremely complicated. Obesity and metabolic factors are apparently involved in the development and progression of this disease process. However, in the present study, ONO-1301 did not affect the body weight, visceral fat weight, blood glucose or total cholesterol level of obese db/db mice.
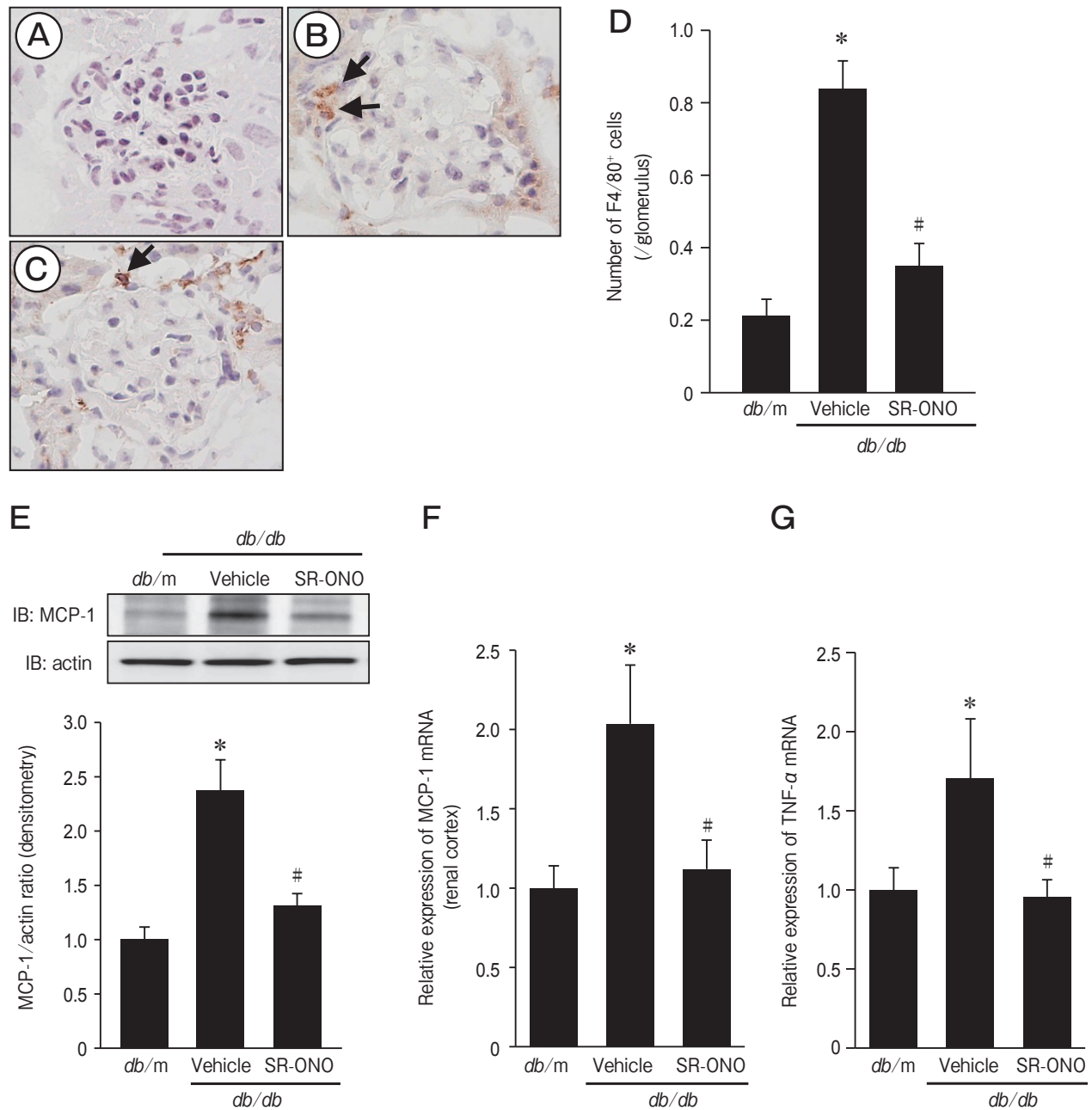
Fig. 5   The infiltration of monocytes/macrophages and the expression of MCP-1 and TNF-α. The glomerular accumulation of F4/80[+] monocytes/macrophages was assessed by an immunohistochemical analysis of the non-diabetic controls (A), diabetic mice treated with vehicle (B), and diabetic mice treated with SR-ONO (C). F4/80^{+} cells were observed in the diabetic mice (arrowheads; original magnification ×400). (D) The numbers of glomerular F4/80[+] monocyte/macrophages are shown. The accumulation of F4/80[+] monocytes/macrophages in the diabetic mice was significantly suppressed by the SR-ONO treatment compared to the vehicle treatment. The expression of MCP-1 was determined by an immunoblot analysis (E) and real-time PCR (F). (G) The expression of TNF-α was determined by real-time PCR. The data are expressed as the values relative to 18S-ribosomal RNA. The data are also expressed as values relative to actin for the immunoblot analyses and 18S-ribosomal RNA for the real-time PCR. *$p < 0.01$ vs. non-diabetic animals. #$p < 0.01$ vs. vehicle-treated diabetic animals. n = 6 in each group. Each column shows the means ± SE.
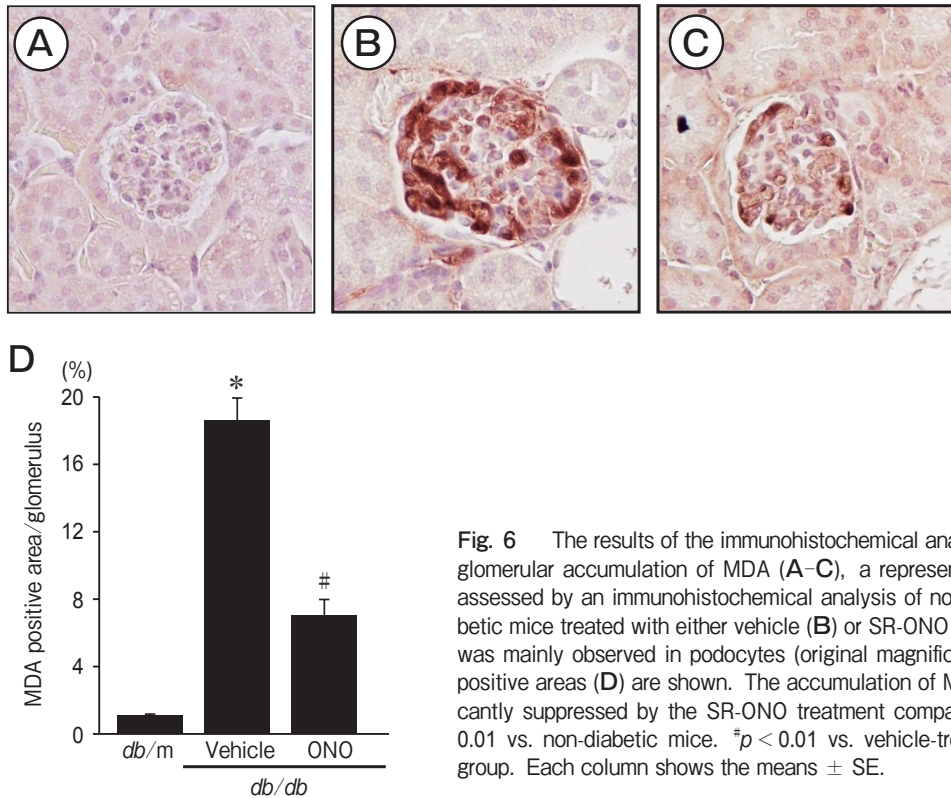
Fig. 6   The results of the immunohistochemical analysis of oxidative stress marker. The glomerular accumulation of MDA (**A–C**), a representative oxidative stress marker, was assessed by an immunohistochemical analysis of non-diabetic control mice (**A**) and diabetic mice treated with either vehicle (**B**) or SR-ONO (**C**). The accumulation of molecules was mainly observed in podocytes (original magnification ×400). The glomerular MDA-positive areas (**D**) are shown. The accumulation of MDA in the diabetic mice was significantly suppressed by the SR-ONO treatment compared to the vehicle treatment. *$p <$ 0.01 vs. non-diabetic mice. #$p < 0.01$ vs. vehicle-treated diabetic mice. n = 6 in each group. Each column shows the means ± SE.

Nonetheless, ONO-1301 reduced the albuminuria and ameliorated the glomerular mesangial expansion in these mice. These are the reasons why we focused on the direct effects of ONO-1301 on glomerular injury in the present study. Glomerular hyperfiltration and glomerular hypertrophy, as well as albuminuria, are characteristic signs of early diabetic nephropathy.

An earlier study suggested that the glomerular size might affect the rate of renal functional decline [39]. ONO-1301 mildly prevented glomerular hypertrophy but not hyperfiltration, as indicated by the increased creatinine clearance, in the diabetic *db/db* mice. These findings are consistent with our previous report of the effects of ONO-1301 treatment in mice with type 1 diabetic nephropathy [17]. A clarification of the potential therapeutic effects of SR-ONO treatment on glomerular hyperfiltration at the higher dosage requires further investigation.

Mesangial cells play a critical role in the pathogenesis of diabetic glomerular injury. Hyperglycemia stimulates this type of cells to exhibit a fibroblast-like phenotype and express α-SMA [2]. These transformed cells produce excessive ECM molecule, such as collagen and fibronectin, and they promote the replacement of the normal tissue with fibrous tissue, leading to glomerulosclerosis. In a previous study in humans, the degree of mesangial matrix expansion correlated with the decrease in the glomerular capillary filtration surface area [40]. Beneficial effects of ONO-1301 on mesangial cells were observed in the present study. ONO-1301 reduced the accumulation of mesangial matrix, which was associated with a decreased level of renal TGF-β expression (Fig. 9). Such effects are consistent with the previous reports of anti-fibrotic effects of ONO-1301 in experimental models of pulmonary fibrosis and renal tubulointerstitial fibrosis [10, 18].

The infiltration of monocytes/macrophages into glomeruli is also involved in the progression of diabetic nephropathy. In this study, ONO-1301 attenuated the glomerular infiltration of monocytes/macrophages in diabetic mice (Fig. 9). This beneficial effect of ONO-1301 was associated with a reduction of glomerular oxidative stress (Fig. 9). In another study, anti-inflammatory effects of a prostacyclin analogue, beraprost sodium, were demonstrated in a model of
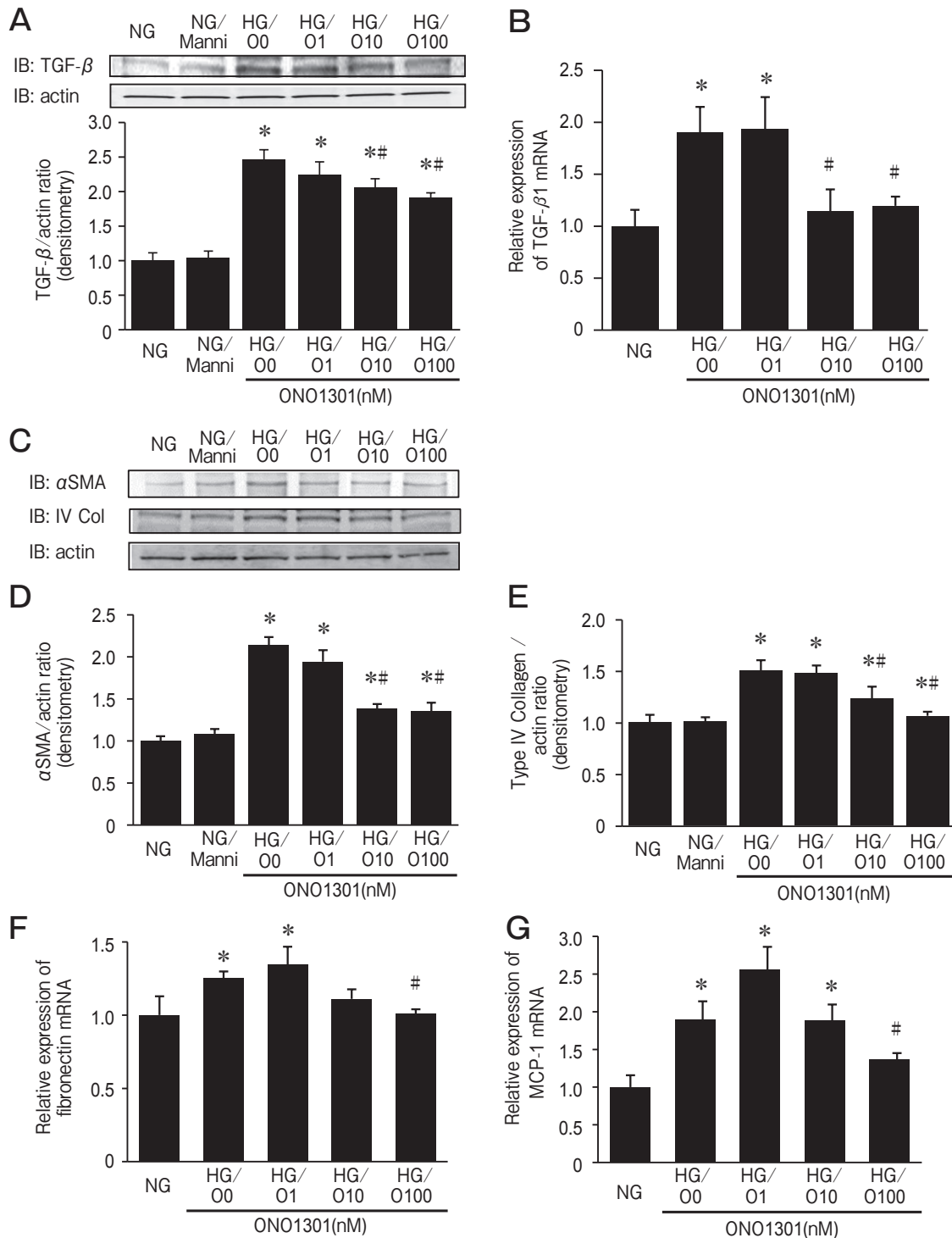
Fig. 7   The inhibitory effects of ON-1301 on the expression of representative mediators involved in fibrosis and inflammation in mouse mesangial cells cultured in normal glucose (NG) or high-glucose (HG) medium. Immunoblotting and real-time PCR analyses demonstrated that the HG-induced upregulation of TGF-β protein (**A**) and mRNA (**B**), α-SMA (**C**, **D**), type IV collagen (**C**, **E**), fibronectin (**F**) and MCP-1 (**G**) were significantly suppressed by ONO-1301. The data are expressed as values relative to actin for the immunoblots and 18S-ribosomal RNA for the real-time PCR. $^{*}p < 0.01$ vs. NG. $^{\#}p < 0.01$ vs. HG. n = 5 in each group. Each column shows the means $\pm$ SE.
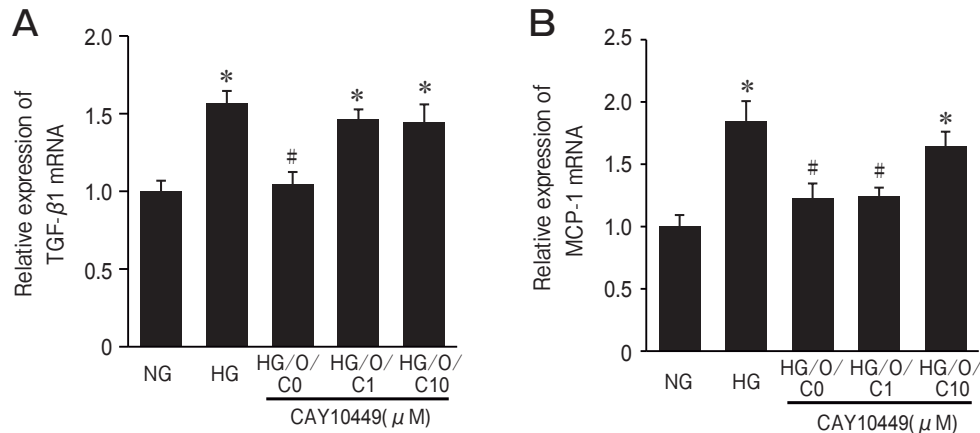
Fig. 8 The results of the qPCR analysis of the mRNA levels of TGF-β1 (**A**) and MCP-1 (**B**) in cultured mouse mesangial cells (Mes13 cells). Cells cultured in high-glucose (HG) medium were treated with ONO-1301 in the presence or absence of a PGI$_2$ (IP) receptor antagonist, CAY10449. The inhibitory effects of ONO-1301 on the expression of both TGF-β and MCP-1 were significantly reversed by concurrent treatment with CAY10449. The data are expressed as values relative to 18S-ribosomal RNA. $^*p < 0.01$ vs. NG. $^{\#}p < 0.01$ vs. HG. n = 5 in each group. Each column shows the means $\pm$ SE.

diabetic nephropathy, and the effects were found to be related to a decreased expression of glomerular intercellular adhesion molecule-1 (ICAM-1) [35]. In the present study, however, ONO-1301 was shown to suppress the expression of MCP-1, a chemokine that contributes to the recruitment of monocytes/macrophages.

The importance of MCP-1 in the development of type 2 diabetic nephropathy was demonstrated in a study of MCP-1 knockout *db/db* mice [41]. Other studies also revealed an association between the infiltration of monocytes/macrophages and the accumulation of the mesangial matrix in models of diabetes [42]. Considering that MCP-1 is a target for various therapeutic agents (including statins and thiazolidinediones) associated with diabetic nephropathy, the potent suppression of MCP-1 expression may be one of the major mechanisms by which ONO-1301 prevented the glomerular injuries in the present study (Fig. 9).

The specific signaling mechanisms by which ONO-1301 exerts its beneficial effects have been studied in a variety of *in vivo* and *in vitro* models. The PGI$_2$ (IP) receptor plays central roles in such signaling pathways. It has been demonstrated that ONO-1301 directly interacts with the IP receptor, and its major downstream effects have been considered to be an increased level of cyclic AMP and the production of HGF [15, 43]. Our previous investigation showed that ONO-1301 suppressed the tubulointerstitial
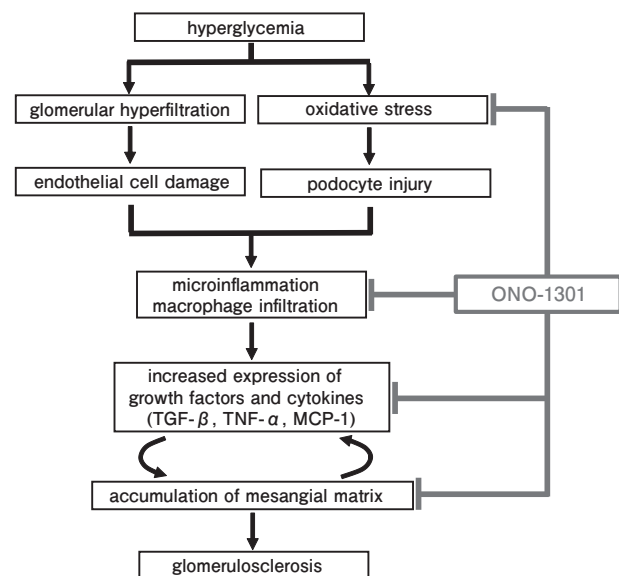

Fig. 9 Schema for the potential therapeutic mechanisms of ONO-1301 against diabetic nephropathy.

injury in a mouse model of unilateral ureteral obstruction, and ONO-1301 suppressed α-SMA expression in cultured proximal tubular cells and maintained the epithelial phenotype via IP receptor signaling [18]. Consistent with these findings, blockade of the IP receptor led to the abolishment of the inhibitory effects of ONO-1301 on TGF-β and MCP-1 expression in cultured mesangial cells in the present study.

This result indicates that the IP receptor on these cells may be essential for the therapeutic effects of ONO-1301.

There are several potential limitations associated with the present study. The intermittent administration of SR-ONO at a dose of 10 mg/kg body weight resulted in a sustained elevation of circulating levels of ONO-1301 around the effective therapeutic levels for several weeks, as reported in previous studies using animal models of pulmonary hypertension and in a rat type 1 diabetes model [12, 17]. The dose of SR-ONO used in the present study was determined based on previous studies [10, 17].

Obata *et al.* revealed that the administration of SR-ONO to rats at a dose of 300 mg/kg led to significant hypotension, but no such systemic effects were observed at 100 mg/kg [12]. Further investigation is needed to determine the therapeutic effects of SR-ONO at the higher dosage, since it may lead to greater renoprotective effects in diabetic nephropathy. In addition, the therapeutic effects of SR-ONO were observed in the present study by initiating therapy from the early stage of diabetes, and it is unclear whether it would be effective at a later stage of diabetic nephropathy.

In conclusion, we demonstrated that an intermittent administration of SR-ONO effectively ameliorated the alterations in a mouse model of type 2 diabetic nephropathy, potentially by inhibiting inflammatory cell infiltration and oxidative stress at least partly through the interaction with the IP receptor, and through anti-fibrotic effects. We hope that our present study will eventually lead to the development of novel therapeutic strategies for patients with diabetic nephropathy.

References

1. Gonzalez Suarez ML, Thomas DB, Barisoni L and Fornoni A: Diabetic nephropathy: Is it time yet for routine kidney biopsy? World J Diabetes (2013) 4: 245–255.
2. Makino H, Kashihara N, Sugiyama H, Kanao K, Sekikawa T, Okamoto K, Maeshima Y, Ota Z and Nagai R: Phenotypic modulation of the mesangium reflected by contractile proteins in diabetes. Diabetes (1996) 45: 488–495.
3. Sharma K and Ziyadeh FN: Hyperglycemia and diabetic kidney disease. The case for transforming growth factor-beta as a key mediator. Diabetes (1995) 44: 1139–1146.
4. Brownlee M, Cerami A and Vlassara H: Advanced glycosylation end products in tissue and the biochemical basis of diabetic complications. N Engl J Med (1988) 318: 1315–1321.
5. Qi XM, Wu GZ, Wu YG, Lin H, Shen JJ and Lin SY: Renoprotective effect of breviscapine through suppression of renal macrophage recruitment in streptozotocin-induced diabetic rats. Nephron Exp Nephrol (2006) 104: e147–157.
6. Huijun W, Long C, Zhigang Z, Feng J and Muyi G: Ex vivo transfer of the decorin gene into rat glomerulus via a mesangial cell vector suppressed extracellular matrix accumulation in experimental glomerulonephritis. Exp Mol Pathol (2005) 78: 17–24.
7. Moncada S, Gryglewski R, Bunting S and Vane JR: An enzyme isolated from arteries transforms prostaglandin endoperoxides to an unstable substance that inhibits platelet aggregation. Nature (1976) 263: 663–665.
8. Moncada S and Vane JR: Arachidonic acid metabolites and the interactions between platelets and blood-vessel walls. N Engl J Med (1979) 300: 1142–1147.
9. Kataoka M, Nagaya N, Satoh T, Itoh T, Murakami S, Iwase T, Miyahara Y, Kyotani S, Sakai Y, Kangawa K and Ogawa S: A long-acting prostacyclin agonist with thromboxane inhibitory activity for pulmonary hypertension. Am J Respir Crit Care Med (2005) 172: 1575–1580.
10. Murakami S, Nagaya N, Itoh T, Kataoka M, Iwase T, Horio T, Miyahara Y, Sakai Y, Kangawa K and Kimura H: Prostacyclin agonist with thromboxane synthase inhibitory activity (ONO-1301) attenuates bleomycin-induced pulmonary fibrosis in mice. Am J Physiol Lung Cell Mol Physiol (2006) 290: L59–65.
11. Nakamura K, Sata M, Iwata H, Sakai Y, Hirata Y, Kugiyama K and Nagai R: A synthetic small molecule, ONO-1301, enhances endogenous growth factor expression and augments angiogenesis in the ischaemic heart. Clin Sci (Lond) (2007) 112: 607–616.
12. Obata H, Sakai Y, Ohnishi S, Takeshita S, Mori H, Kodama M, Kangawa K, Aizawa Y and Nagaya N: Single injection of a sustained-release prostacyclin analog improves pulmonary hypertension in rats. Am J Respir Crit Care Med (2008) 177: 195–201.
13. Iwata H, Nakamura K, Sumi M, Ninomiya M, Sakai Y, Hirata Y, Akaike M, Igarashi T, Takamoto S, Nagai R and Sata M: Local delivery of synthetic prostacycline agonist augments collateral growth and improves cardiac function in a swine chronic cardiac ischemia model. Life Sci (2009) 85: 255–261.
14. Hazekawa M, Sakai Y, Yoshida M, Haraguchi T and Uchida T: Single injection of ONO-1301-loaded PLGA microspheres directly after ischaemia reduces ischaemic damage in rats subjected to middle cerebral artery occlusion. J Pharm Pharmacol (2012) 64: 353–359.
15. Uchida T, Hazekawa M, Yoshida M, Matsumoto K and Sakai Y: A Novel Long-Acting Prostacyclin Agonist (ONO-1301) With an Angiogenic Effect: Promoting Synthesis of Hepatocyte Growth

Factor and Increasing Cyclic AMP Concentration via IP-Receptor Signaling. J Pharmacol Sci (2013) 123: 392–401.

16. Hayashi K, Nagamatsu T, Oka T and Suzuki Y: Modulation of anti-glomerular basement membrane nephritis in rats by ONO-1301, a non-prostanoid prostaglandin I2 mimetic compound with inhibitory activity against thromboxane A2 synthase. Jpn J Pharmacol (1997) 73: 73–82.

17. Yamasaki H, Maeshima Y, Nasu T, Saito D, Tanabe K, Hirokoshi-Kawahara K, Sugiyama H, Sakai Y and Makino H: Intermittent administration of a sustained-release prostacyclin analog ONO-1301 ameliorates renal alterations in a rat type 1 diabetes model. Prostaglandins Leukot Essent Fatty Acids (2011) 84: 99–107.

18. Nasu T, Kinomura M, Tanabe K, Yamasaki H, Htay SL, Saito D, Hinamoto N, Watatani H, Ujike H, Suzuki Y, Sugaya T, Sugiyama H, Sakai Y, Matsumoto K, Maeshima Y and Makino H: Sustained-release prostacyclin analog ONO-1301 ameliorates tubulointerstitial alterations in a mouse obstructive nephropathy model. Am J Physiol Renal Physiol (2012) 302: F1616–1629.

19. Imawaka H and Sugiyama Y: Kinetic study of the hepatobiliary transport of a new prostaglandin receptor agonist. J Pharmacol Exp Ther (1998) 284: 949–957.

20. Maeshima Y, Kashihara N, Yasuda T, Sugiyama H, Sekikawa T, Okamoto K, Kanao K, Watanabe Y, Kanwar YS and Makino H: Inhibition of mesangial cell proliferation by E2F decoy oligodeoxynucleotide in vitro and in vivo. J Clin Invest (1998) 101: 2589–2597.

21. Weibel ER: Practical Methods for Biological Morphometry; in Stereological Methods, Vol. 1, R.S. Fritsch eds, Academic Press, London (1979) pp51–57.

22. Nasu T, Maeshima Y, Kinomura M, Hirokoshi-Kawahara K, Tanabe K, Sugiyama H, Sonoda H, Sato Y and Makino H: Vasohibin-1, a negative feedback regulator of angiogenesis, ameliorates renal alterations in a mouse model of diabetic nephropathy. Diabetes (2009) 58: 2365–2375.

23. Ichinose K, Maeshima Y, Yamamoto Y, Kinomura M, Hirokoshi K, Kitayama H, Takazawa Y, Sugiyama H, Yamasaki Y, Agata N and Makino H: 2-(8-hydroxy-6-methoxy-1-oxo-1h-2-benzopyran-3-yl) propionic acid, an inhibitor of angiogenesis, ameliorates renal alterations in obese type 2 diabetic mice. Diabetes (2006) 55: 1232–1242.

24. Tanabe K, Maeshima Y, Ichinose K, Kitayama H, Takazawa Y, Hirokoshi K, Kinomura M, Sugiyama H and Makino H: Endostatin peptide, an inhibitor of angiogenesis, prevents the progression of peritoneal sclerosis in a mouse experimental model. Kidney Int (2007) 71: 227–238.

25. Yamamoto Y, Maeshima Y, Kitayama H, Kitamura S, Takazawa Y, Sugiyama H, Yamasaki Y and Makino H: Tumstatin peptide, an inhibitor of angiogenesis, prevents glomerular hypertrophy in the early stage of diabetic nephropathy. Diabetes (2004) 53: 1831–1840.

26. Saito D, Maeshima Y, Nasu T, Yamasaki H, Tanabe K, Sugiyama H, Sonoda H, Sato Y and Makino H: Amelioration of renal alterations in obese type 2 diabetic mice by vasohibin-1, a negative feedback regulator of angiogenesis. Am J Physiol Renal Physiol (2011) 300: F873–886.

27. Ichinose K, Maeshima Y, Yamamoto Y, Kitayama H, Takazawa Y, Hirokoshi K, Sugiyama H, Yamasaki Y, Eguchi K and Makino H: Antiangiogenic endostatin peptide ameliorates renal alterations in the early stage of a type 1 diabetic nephropathy model. Diabetes (2005) 54: 2891–2903.

28. Maeshima Y, Sudhakar A, Lively JC, Ueki K, Kharbanda S, Kahn CR, Sonenberg N, Hynes RO and Kalluri R: Tumstatin, an endothelial cell-specific inhibitor of protein synthesis. Science (2002) 295: 140–143.

29. Awad AS, Ye H, Huang L, Li L, Foss FW, Jr., Macdonald TL, Lynch KR and Okusa MD: Selective sphingosine 1-phosphate 1 receptor activation reduces ischemia-reperfusion injury in mouse kidney. Am J Physiol Renal Physiol (2006) 290: F1516–1524.

30. Maeshima Y, Kashihara N, Sugiyama H, Makino H and Ota Z: Antisense oligonucleotides to proliferating cell nuclear antigen and Ki-67 inhibit human mesangial cell proliferation. J Am Soc Nephrol: JASN (1996) 7: 2219–2229.

31. Sharma K, Jin Y, Guo J and Ziyadeh FN: Neutralization of TGF-beta by anti-TGF-beta antibody attenuates kidney hypertrophy and the enhanced extracellular matrix gene expression in STZ-induced diabetic mice. Diabetes (1996) 45: 522–530.

32. Iehara N, Takeoka H, Tsuji H, Imabayashi T, Foster DN, Strauch AR, Yamada Y, Kita T and Doi T: Differentiation of smooth muscle phenotypes in mouse mesangial cells. Kidney Int (1996) 49: 1330–1341.

33. Johnson G, 3rd, Furlan LE, Aoki N and Lefer AM: Endothelium and myocardial protecting actions of taprostene, a stable prostacyclin analogue, after acute myocardial ischemia and reperfusion in cats. Circ Res (1990) 66: 1362–1370.

34. McLaughlin VV, Genthner DE, Panella MM and Rich S: Reduction in pulmonary vascular resistance with long-term epoprostenol (prostacyclin) therapy in primary pulmonary hypertension. N Engl J Med (1998) 338: 273–277.

35. Yamashita T, Shikata K, Matsuda M, Okada S, Ogawa D, Sugimoto H, Wada J and Makino H: Beraprost sodium, prostacyclin analogue, attenuates glomerular hyperfiltration and glomerular macrophage infiltration by modulating ecNOS expression in diabetic rats. Diabetes res clin prac (2002) 57: 149–161.

36. Watanabe M, Nakashima H, Mochizuki S, Abe Y, Ishimura A, Ito K, Fukushima T, Miyake K, Ogahara S and Saito T: Amelioration of diabetic nephropathy in OLETF rats by prostaglandin I(2) analog, beraprost sodium. Am j nephrol (2009) 30: 1–11.

37. Xu S, Jiang B, Maitland KA, Bayat H, Gu J, Nadler JL, Corda S, Lavielle G, Verbeuren TJ, Zuccollo A and Cohen RA: The thromboxane receptor antagonist S18886 attenuates renal oxidant stress and proteinuria in diabetic apolipoprotein E-deficient mice. Diabetes (2006) 55: 110–119.

38. Sebekova K, Eifert T, Klassen A, Heidland A and Amann K: Renal effects of S18886 (Terutroban), a TP receptor antagonist, in an experimental model of type 2 diabetes. Diabetes (2007) 56: 968–974.

39. Bilous RW, Mauer SM, Sutherland DE and Steffes MW: Mean glomerular volume and rate of development of diabetic nephropathy. Diabetes (1989) 38: 1142–1147.

40. Ellis EN, Steffes MW, Goetz FC, Sutherland DE and Mauer SM: Glomerular filtration surface in type I diabetes mellitus. Kidney Int (1986) 29: 889–894.

41. Chow FY, Nikolic-Paterson DJ, Ma FY, Ozols E, Rollins BJ and Tesch GH: Monocyte chemoattractant protein-1-induced tissue inflammation is critical for the development of renal injury but not type 2 diabetes in obese db/db mice. Diabetologia (2007) 50: 471–480.

42. Sassy-Prigent C, Heudes D, Mandet C, Belair MF, Michel O, Perdereau B, Bariety J and Bruneval P: Early glomerular macrophage recruitment in streptozotocin-induced diabetic rats. Diabetes (2000) 49: 466–475.

43. Mizuno S and Nakamura T: Suppressions of chronic glomerular injuries and TGF-beta 1 production by HGF in attenuation of murine diabetic nephropathy. Am J Physiol Renal Physiol (2004) 286: F134–143.